RSC Advances

PAPER

View Article Online
View Journal | View Issue

Cite this: *RSC Adv.*, 2024, **14**, 31663

Synthesis of a novel carbon-based nano-emulsifier and its application in viscosity reduction of emulsified Jurassic oil in the Sichuan Basin

Weihua Chen,[a] Rui He,[a] Rui Liu, *[bc] Ji Zeng,[a] Ruifeng Liu,[bd] Hancheng Wang,[a] Wenting Guan,[a] Zefei Lv,[a] Bingjie Fu[bc] and Wanfen Pu[bc]

A study was undertaken into the emulsification and viscosity reduction processes of crude oil originating from the Jurassic formation of the Sichuan Basin. Central to this investigation was the successful synthesis of a carbon-based nano emulsifier named GOPH, utilizing graphene oxide as substrate and hydrophilic alkyl glycidyl ether and polyoxyethylene ether as modifiers. The structural integrity of this nano-emulsifier was comprehensively characterized *via* Fourier transform infrared spectroscopy, scanning electron microscopy, and thermogravimetric analysis. Notably, GOPH nanofluids exhibited a remarkable merit in decreasing the oil/water interfacial tension from 31.96 mN m^{-1} to a low value of 9.76 mN m^{-1} with a critical concentration of 45 ppm. Moreover, interfacial film folding experiments revealed that GOPH nanoparticles "jammed" at the oil–water interface, forming a robust film. When Jurassic crude oil was the oil phase, and GOPH nanofluids were introduced into the water phase, the crude oil was successfully induced to form a low-viscosity oil-in-water (O/W) emulsion. Emulsion droplet size and viscosity measurements demonstrated that this emulsion possessed small size distributions with remarkable stability, achieving a viscosity reduction of up to 91.6% at a water content of 80%. The underlying mechanism for this phenomenon mainly lies in the interaction between the carbon-based nano-emulsifier and asphaltene, which form a composite unit, enabling the construction of a flexible interfacial film that significantly stabilizes the O/W emulsion.

Received 17th July 2024
Accepted 1st October 2024

DOI: 10.1039/d4ra05188b

rsc.li/rsc-advances

1. Introduction

Despite the global momentum toward renewable and environmentally friendly energy sources, crude oil remains pivotal in fulfilling the world's energy demands. Crude oil is an efficient and reliable energy resource that is indispensable for global economic progress and social development.[1] Nevertheless, crude oil produced from the Jurassic formations in Sichuan Basin encounters distinct challenges due to its high concentration of heavy fractions, such as asphaltenes and colloids, which significantly increase the viscosity of crude oil. The high viscosity of the crude oil results in the unfavorable mobility between the displacing phase (water) and the displaced phase (crude oil) causing severe viscous finger and tongue phenomena in porous media during the water flooding process. It is clear that the sweep volume of the injected water is small and a large amount of crude oil remains underground even after extensive water flooding process.[2–5] To address this challenge, various enhanced oil recovery (EOR) methods were developed, such as thermal and chemical processes.[6–11] Thermal EOR, while effectively extracting high-viscosity crude oil by decreasing the viscosity of crude oil in the formation, may confront significant challenges regarding high energy consumption and potential environmental impacts. The viscosity reduction technology concerning crude oil emulsification in the formation is a promising chemical enhanced oil recovery (CEOR) method.[12–14] This technology stands out due to its versatility, simplicity, and cost-effectiveness. Introducing a small amount of emulsifier into crude oil transforms into oil-in-water emulsions, effectively reducing viscosity by several orders of magnitude. Given the challenge posed by crude oil from Jurassic formations in the Sichuan Basin, the viscosity reduction technology through crude oil emulsification offers an attractive solution for EOR, and the performance of emulsifier is critical.

Viscosity reduction technology through crude oil emulsification using surfactant has emerged as a prevalent approach in chemical oil recovery. The efficacy of surfactants is attributed to their distinctive amphiphilic nature, which comprises both hydrophobic and hydrophilic moieties, enabling their adsorption

[a]*Engineering Technology Research Institute, PetroChina Southwest Oil & Gasfield Company, Chengdu, Sichuan, 610017, China. E-mail: chen_weihua@petrochina.com.cn; herui6868@163.com; zeng_ji@petrochina.com.cn; wanghancheng@petrochina.com.cn; guanwenting@petrochina.com.cn; lvzefei@petrochina.com.cn*

[b]*State Key Laboratory of Oil and Gas Reservoir Geology and Exploitation, Southwest Petroleum University, Chengdu, 610500, China. E-mail: swpuliur@swpu.edu.cn; pwf58@163.com; 59140582@qq.com; liuruifengtroy@163.com*

[c]*Tianfu Yongxing Laboratory, Chengdu, 610213, China*

[d]*CNOOC Guangdong Natural Gas Co., Ltd., Zhuhai, 519015, China*

at the oil–water interface. Consequently, surfactants facilitate formation of stable, oil-in-water (O/W) emulsions with low-viscosity that exhibit favorable mobility through porous media, ultimately enhancing oil recovery.[15–17] However, it is noteworthy that the effective concentration of surfactant is usually diminished due to adsorption onto the rock surface.[18–20] The use of innovative materials might offer a promising path to more efficient and sustainable chemical oil recovery technologies.[21,22]

With the deepening of research, nanotechnology has attracted significant attention from researchers in the oil and gas industry in recent years.[23] Nanoparticles, serving as the core carrier of nanotechnology, possess numerous unique properties, including a high specific surface area, exceptional chemical reactivity, and an active surface.[24] These attributes contribute to the widespread application of nanoparticles in the petroleum industry. In recent years, novel types of "smart fluids" or nanofluids formulated with nanoparticles and base fluids have emerged as prominent candidates for use in the petroleum industry.[25,26] These innovative fluids are deliberately designed to enhance specific fluid properties by adding nanoparticles, ultimately aiming to improve oil recovery. Incorporating specific nanoparticles into the injected solution has demonstrated remarkable performance in enhancing oil recovery compared to traditional surfactants. The advantages of using nanoparticles are multifaceted. They can modify the properties of fluids, such as reducing the interfacial tension (IFT), thereby improving the mobility of trapped oil and enhancing oil repulsion. Moreover, nanoparticles act as emulsifiers to induce the formation of oil-in-water emulsions, thereby significantly improving the mobility of crude oil.[27–32]

Saigal[33] successfully created a range of emulsion stabilizers for xylene-in-water and cyclohexane-in-water systems by decorating silica nanoparticles with poly(2-(dimethylamino)ethyl methacrylate) using atom-transfer radical polymerization. Their research revealed that the emulsifier with the most effectiveness and stability had a grafting density of 0.077 chains per nm^2. Notably, they found that a mass concentration of just 500 ppm of these particles was sufficient to stabilize the oil-in-water emulsions. Khoramian[34] observed an intriguing phenomenon where the presence of graphene oxide (GO) significantly reduced the interfacial tension between oil and water in various concentrations of NaCl solutions. This reduction in interfacial tension facilitated the formation of a more stable emulsion with crude oil, leading to a notable 28% increase in oil recovery rates in micro-model flooding experiments. Chen[35] introduced a novel amphiphilic graphene oxide (H-GO) exhibiting exceptional emulsification properties. Their study revealed that the Pickering emulsions stabilized by H-GO possessed a diameter of approximately 2.66 μm and demonstrated remarkable stability. Moreover, the researchers aimed to design a screening criterion that would facilitate the identification of nanoparticles as potential emulsifiers for heavy oils, which represents a significant advance in this field. On the other hand, a different strategy was proposed by synthesizing amphiphilic graphene oxide (GOA) and graphene oxide for liquid crystal (GOC) through chemical modifications of GO. Their comprehensive interfacial experiments and molecular dynamics simulations revealed that GOA and GOC spontaneously accumulate at the oil–water interface, forming robust interfacial films that significantly enhance crude oil recovery.[36] Despite profound potential for nanofluids to reduce crude oil viscosity and optimize underground emulsification, there are still crucial gaps in understanding. Specifically, there is an urgent need to elucidate fundamental issues such as the precise role of nanofluids at the water/oil interface and the mechanisms underlying their influence on oil-in-water emulsions.

Here, we report the successful preparation of a novel carbon-based nano-emulsifier called GOPH, utilizing graphene oxide as the core material, and augmenting its properties with hydrophilic alkyl glycidyl ether and poloxamer modifiers. In the functionalization of graphite oxide, alkyl glycidyl ethers exhibit hydrophilic and hydrophobic properties stemming from their molecular ether and alkyl groups, respectively. Concurrently, poloxamer, a surfactant renowned for its low toxicity and high biocompatibility, attracts significant interest in graphite oxide modification.[37] Composed of a PEO-PPO-PEO triblock copolymer, poloxamer manifests unique amphiphilicity. We conducted a systematic evaluation of interfacial properties to elucidate the emulsification and viscosity reduction capabilities of GOPH nanofluids. A comprehensive experiments encompassing interfacial tension measurements, emulsification capacity assessments, emulsion droplet size distribution analysis, emulsion viscosity measurements, stability tests, and rheological characterization were undertaken to reveal the viscosity reduction mechanism of the crude oil induced by GOPH nanofluids. The outcomes of these experiments offer profound insights into how GOPH nanoparticles interact with crude oil and water interfaces, promote the formation of oil-in-water emulsions. The findings in this study would provide valuable references and experimental support for crude oil emulsification and viscosity reduction *via* nanotechnology.

2. Experimental section

2.1 Materials

The GO, purchased from Aladdin Reagent (Shanghai), with an average size of 8000 mesh. Poloxamer and hydrophilic alkyl glycidyl with 98% purity were obtained from Shanghai Yi En Chemical Technology Co., Ltd and Chengdu Kelong Chemical Reagent Co., Ltd, respectively. The crude oil used for the experiment was from one block of PetroChina Southwest Oil & Gas field, with a density of 0.84 g cm^{-3} and a viscosity of 10.16 mPa s at 70 °C. The properties and SARA (saturates, aromatics, resins, and asphaltenes) composition of the crude oil are listed in Table 1. Here, the density was determined by the mass-volume method, and the viscosity was also determined by a Brookfield DVIII Pro rotational viscometer.

The formation water was filtered using a membrane to remove mechanical impurities, and the total mineralization was 34 737.8 mg L^{-1}. The ionic compositions of the formation water are shown in Table 2.

2.2 Preparation of GOPH nanofluids

The GOPH, a modified carbon-based nano-emulsifier, was successfully synthesized using graphene oxide (GO) as

Table 1 Composition and properties of crude oil (70 °C)

Density@70 °C ($g\ cm^{-3}$)	Viscosity@70 °C (mPa s)	SARA (%)			
		Resins	Asphaltenes	Saturates	Aromatics
0.84	10.16	25.1	4.8	25.6	42.1

Table 2 Ion composition of formation water

	Ion content ($mg\ L^{-1}$)							
Water sample	HCO_3^-	Cl^-	CO_3^{2-}	SO_4^{2-}	Ca^{2+}	Mg^{2+}	$Na^+ + K^+$	Total salinity
Formation water	11834	8030.1	564	1264.2	696	146.4	12203.1	34737.8

substrate. At the beginning of synthesis, 5 g of hydrophilic alkyl glycidyl ether and 5 g of poloxamer were accurately weighed in a glass container. This mixture was then transferred to a reactor equipped with a stirrer, where the temperature was elevated to 80 °C, and subjected to agitation for 15 minutes to facilitate thorough dissolution. Subsequently, following adequate stirring, 0.5 g of graphene oxide was carefully introduced into this reactor. The reactor was then positioned within a muffle and heated to 200 °C for 2 hours. After the reaction is completed, the system was allowed to cool to ambient temperature. The product resulting from the reaction was purified using anhydrous ethanol. Finally, the blackened product underwent further drying and grinding procedures to produce the desired modified carbon-based nano-emulsifier, GOPH. The schematic diagram of synthetic route for generating GOPH is depicted in Fig. 1a. In this study, a two-step method was employed to prepare carbon-based nanofluids, considering the individual synthesis of carbon-based nano-emulsifiers. A precise quantity of GOPH nanoparticles was introduced into groundwater and agitated in a beaker to ensure homogeneity. Subsequently, the resulting mixture underwent preliminary mixing using a magnetic stirrer to obtain initial GOPH dispersion in the formation water. Finally, the nanofluids were transferred to an ultrasonic cleaner for sonication, a step that further enhanced the dispersion and stability of the nanoparticles. Fig. 1b provides a detailed step for the preparation of carbon-based nanofluids.

2.3 Characterization of GOPH

A Fourier transform infrared (FTIR) spectrometer (Thermo Scientific, USA) was employed for the analysis of functional groups of GOPH. Thermogravimetry (TGA) was obtained by raising the temperature from room temperature to 800 °C in a rate of 10 °C min^{-1} in nitrogen atmosphere. The stability of the GOPH nanofluids samples was determined over a long period of time at 90 °C. The morphology of GOPH was measured using a benchtop scanning electron microscope (SEM) from Thermo Scientific (The Netherlands). A German SDT spin-drop IFT meter (Fig. 2a) was selected to measure the dynamic IFT between the crude oil and the GOPH nanofluids. Before measuring the IFT, the density of the crude oil and GOPH nanofluids needed to be analyzed. Throughout the test, the temperature was set to 70 °C, which corresponds to the temperature in the reservoir. A minimum of 60 min of measurement was required until the IFT data was stable. The wetting contact angle of the initial state of the natural rocks was also tested using the Krüss DSA100 pendant drop method (Fig. 2b). These natural rock slices were placed into bottles filled with GOPH nanofluids and the bottles were aged at 70 °C. These core slices were taken out of the bottles to measure the three-phase contact angles at different time of the immersion (1, 3, 5, 7, and 14 days). The DSA100 Droplet Shape Analyzer was also used to measure the interfacial behavior of GOPH nanofluids. Droplets containing 800 ppm of the GOPH nanofluids were suspended in the oil phase and left to stand for about 30 min. Subsequently, the droplet size was varied by squeezing and sucking processes to observe the wrinkling and flexing process of the interfacial film.

2.4 Preparation of emulsions

The viscosity reduction performance of crude oil induced by GOPH nanofluids was investigated by preparing oil-in-water (O/W) emulsions. Mixtures of crude oil and GOPH nanofluids were prepared with different water contents and placed in a customized measuring cylinder with a total volume of 30 mL at 70 °C. The mixture was stirred with FH-200-HS emulsifier with a shear time of 30 min at 3500 rpm. Crude oil and formation water (without the addition of GOPH nanoparticles) was emulsified under the same emulsification conditions described above.

2.5 Morphology and droplet size distribution of emulsions

The morphology and droplet size distribution are important to the evaluation of emulsions. A DMLB2 Leica microscope (Germany GmbH) was used to observe the microscopic images and distribution of the emulsion. Droplet size histograms were analyzed using ImageJ software (National Institutes of Health, USA). The average droplet size d_{50} was obtained using the arithmetic mean method.

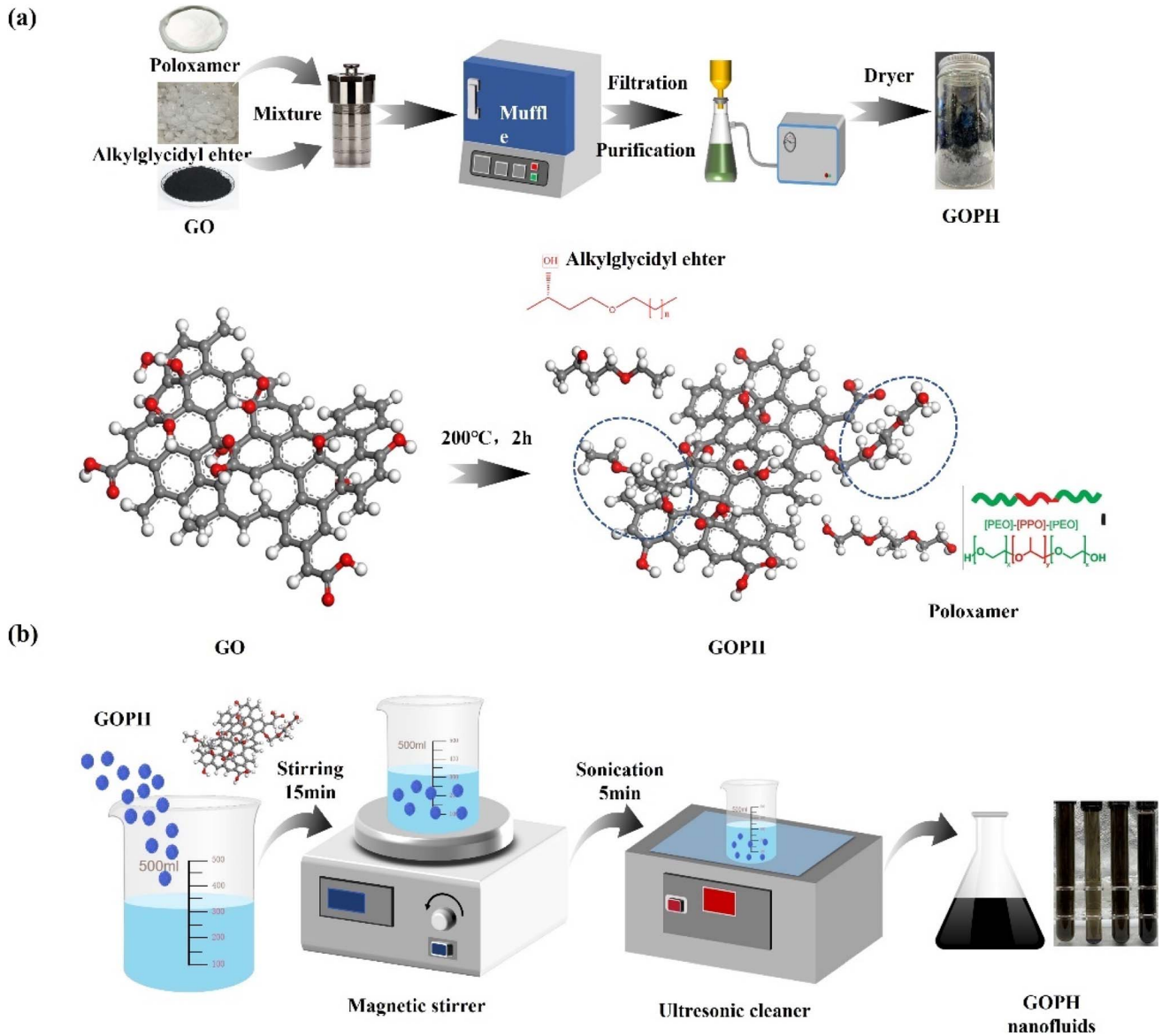

Fig. 1 Schematic diagram of the synthetic route of GOPH (a) and process diagram of preparation of GOPH nanofluids (b).

2.6 Measurement of viscosity, stability and viscoelastic properties of emulsion

The apparent viscosity of emulsions was measured using a Brookfield DVIII Pro rotational viscometer at the reservoir temperature of 70 °C. The stability of the emulsion was studied at 70 °C, and the corresponding dewatering rate was recorded. The viscoelasticity of emulsions was determined using the pendant method of the Krüss DSA 100 droplet shape analyzer. The modulus of dilatancy was measured by sinusoidal variation of the droplet area at a set amplitude and frequency. The droplet shape analysis program was used for image analysis, and the droplet shape was processed based on the fundamental equation of Young Laplace. The amplitude was 100%, the frequency range was 0.1–100 Hz. All samples were repeated at least three times to ensure reproducibility.

3. Results and discussion

3.1 Characterization of GOPH

The thermal stability of the carbon-based nano-emulsifier GOPH was assessed *via* thermogravimetric analysis conducted under a nitrogen atmosphere. As depicted in the TG (thermogravimetric, red curve) and DTG (derivative thermogravimetric, blue curve) curves in Fig. 3a, the pyrolysis process of GOPH can be broadly categorized into three distinct stages. The initial stage, from 70 °C to 120 °C, corresponds to the dry dehydration process, where a significant weight loss is observed primarily due to the evaporation of free and bound water. The subsequent stage, ranging from 220 °C to 500 °C, represents the main pyrolysis process. Here, the TG curve exhibits a steep decline, while the DTG curve displays a pronounced peak in the weight loss rate. This trend is attributed to the pyrolysis of

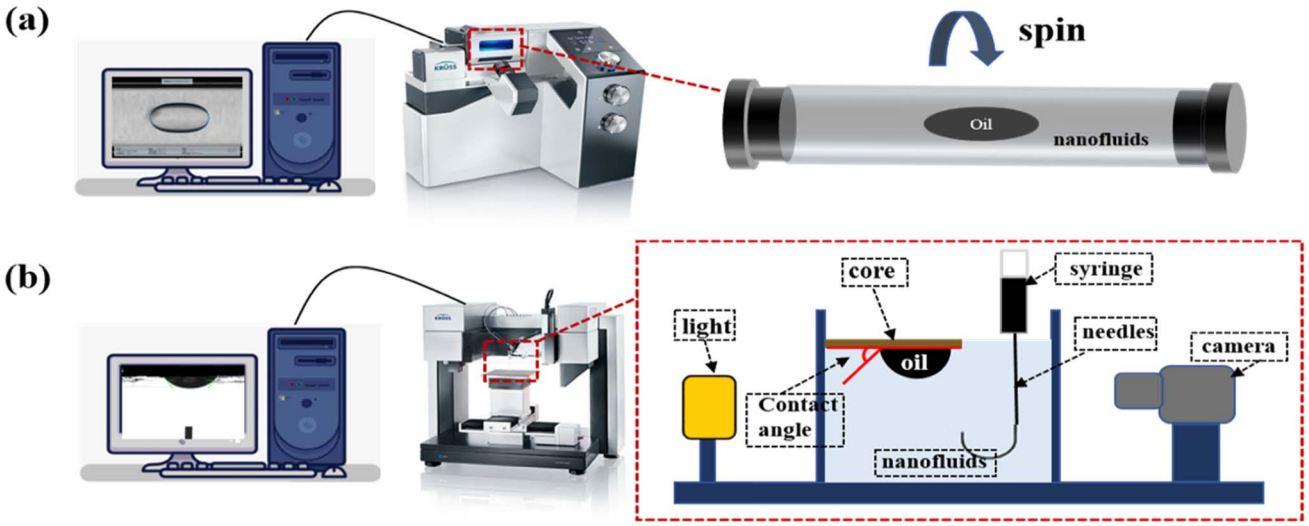

Fig. 2 Schematic diagrams of (a) interfacial tension and (b) contact angle measurement devices.

chemical bonds within GOPH, leading to alterations in its molecular structure and influencing its thermal stability. The final stage, extending from 500 °C to 800 °C, represents the carbonization of the residue. As the temperature surpasses the decomposition threshold, the mass of GOPH gradually decreases with increasing temperature. This moisture loss can

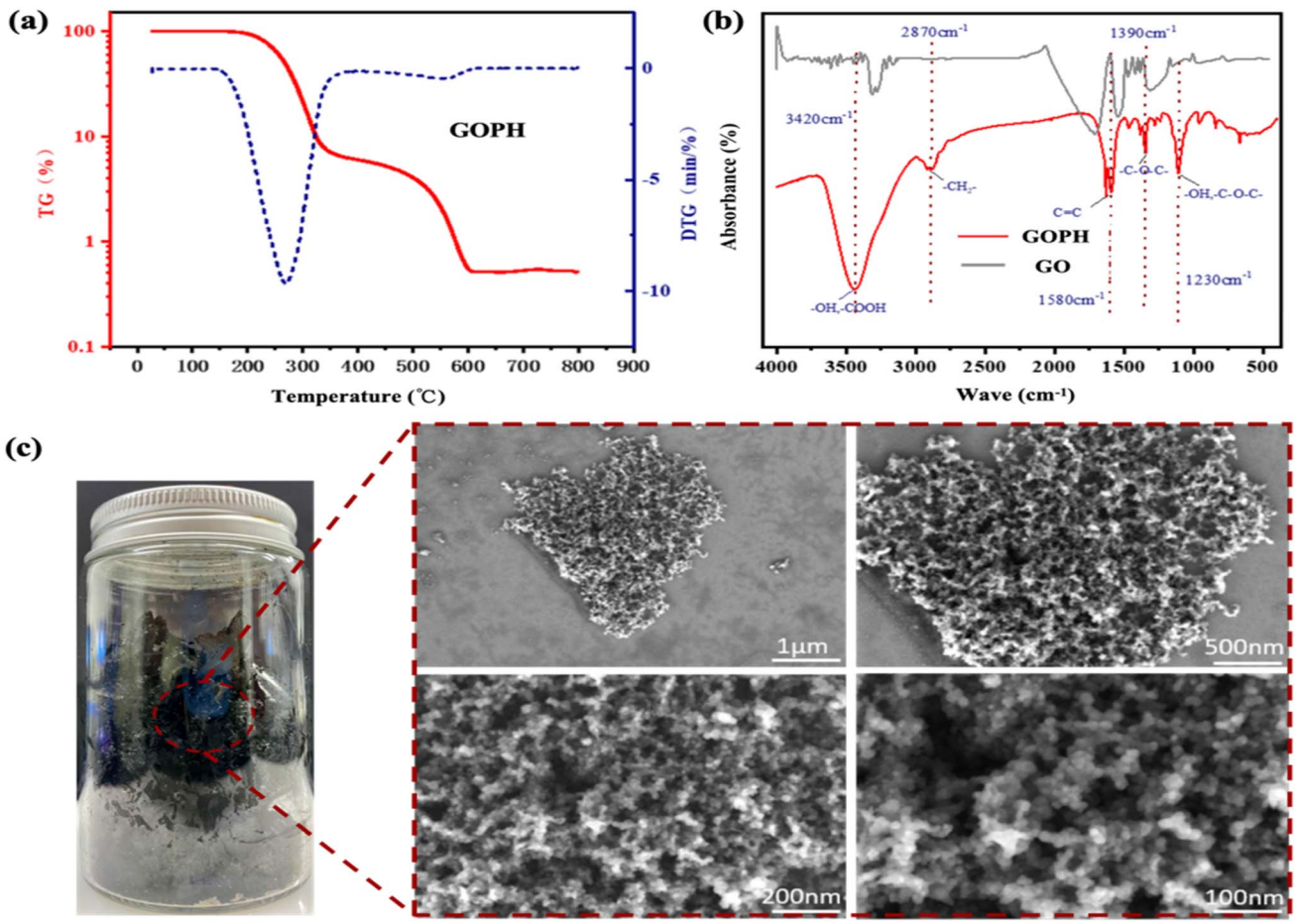

Fig. 3 (a) TG and DTG curves of GOPH nanoparticles under nitrogen atmosphere. (b) Infrared spectra of GOPH and (c) microscopic morphology of dry GOPH.

potentially compromise the three-dimensional structural integrity of GOPH.

Fig. 3b presents the Fourier transform infrared (FTIR) spectra of the GOPH surface before and after modification. A prominent absorption peak at 3420 cm^{-1} indicates the stretching of hydroxyl (hydroxy-OH) and carboxyl (carboxy-COOH) groups in GOPH. The peak around 1640 cm^{-1} corresponds to the stretching vibration of C–C bonds and the vibrational mode of adsorbed water. The peak at 2870 cm^{-1} is attributed to the rocking vibration of methylene ($-CH_2-$) groups and the bending vibration of hydroxyl (–OH) groups. The absorption peak at 1580 cm^{-1} is associated with the C=C aromatic group. Additionally, firm absorption peaks at 1390 cm^{-1} and 1230 cm^{-1} are observed, which can be ascribed to the –OH hydroxyl group and the –C–O–C-vinyl ether moiety, respectively. During the synthesis process, these peaks likely originate from the reaction between hydrophilic hydroxyl groups of alkyl glycidyl ether, poloxamer, and graphene oxide. These findings validate the successful synthesis of GOPH. Notably, Fig. 3c offers a visual representation of the microscopic morphology of the dry GOPH nanoparticles, revealing its characteristic of two-dimensional lamellar structure.

3.2 Interface properties of GOPH nanofluids

GOPH nanoparticles exhibit a spontaneous ability to adsorb at the air–water interface stemming from the amphiphilic nature of the molecule. Specifically, the hydrophilic terminus of GOPH spontaneously extends into the aqueous phase, while the carbonyl end of the graphene oxide remains exposed to air. As depicted in Fig. 4a, a gradual increase in GOPH nanoparticles concentration leads to a rapid decrease in the surface tension. The surface tension reaches a plateau at the GOPH concentration of 45 ppm, indicating the critical concentration of GOPH. Notably, the concentration of GOPH at this interface is relatively modest, and further increment in GOPH concentration yields only marginal reduction in surface tension. Fig. 4a demonstrates that even at low level concentrations, GOPH have a remarkable efficacy in reducing surface tension.

GOPH nanofluids at the concentration of 50 ppm were prepared with formation water. The dynamic interfacial tension data between GOPH nanofluids and simulated oil (white oil, which is mainly composed of hydrocarbon compounds such as alkanes, cycloalkanes and a small amount of aromatic hydrocarbons) or crude oil is presented in Fig. 4b. We noted that in the initial state, the oil–water interfacial tension between crude oil and formation water was 31.96 mN m^{-1}, while that was 35.68 mN m^{-1} between simulated oil and formation water. A substantial reduction in interfacial tension was observed upon the addition of GOPH to these systems. Specifically, the interfacial tension between crude oil and formation water significantly decreased from 31.96 mN m^{-1} to 9.76 mN m^{-1}, and the interfacial tension between simulated oil and formation water was also decreased to 16.18 mN m^{-1}.

Fig. 5 depicts the evolution of equilibrium interfacial tensions between GOPH nanofluids and simulated oil or crude oil as functions of GOPH concentration. At low GOPH concentration (below 300 ppm), the introduction of GOPH significantly influenced the reduction in interfacial tension (IFT). At the GOPH concentration around 300 ppm, the IFT achieved the lowest value that is 4.95 mN m^{-1} for crude oil, and 14.86 mN m^{-1} for simulated oil, respectively. This phenomenon likely arises from the lipophilic and hydrophilic moieties of GOPH, which enable it to form a thin film at the oil–water interface, reducing the IFT. As the concentration of GOPH increased beyond 300 ppm, the IFT continued to display a declining trend at a more gradual rate. Notably, the interfacial tension between GOPH and crude oil consistently remained lower than that of GOPH nanofluids and simulated oil. This discrepancy may stem from the natural active components of crude oil, such as

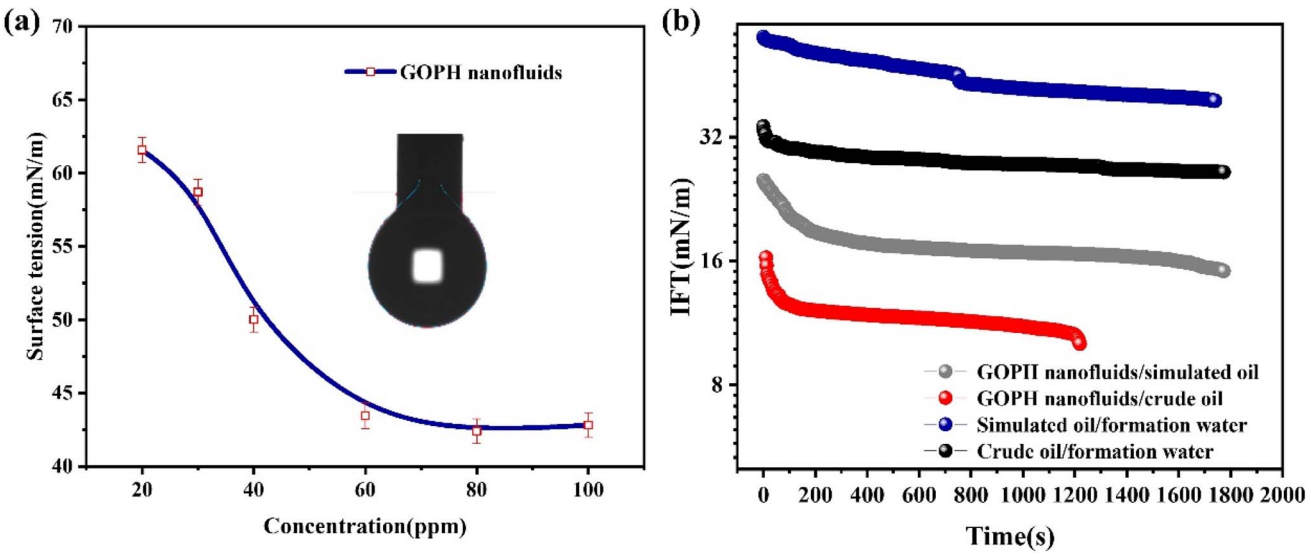

Fig. 4 (a) Equilibrium surface tension of GOPH nanofluids with different concentrations, (b) dynamic interfacial tensions between GOPH nanofluids and simulated oil/crude oil.

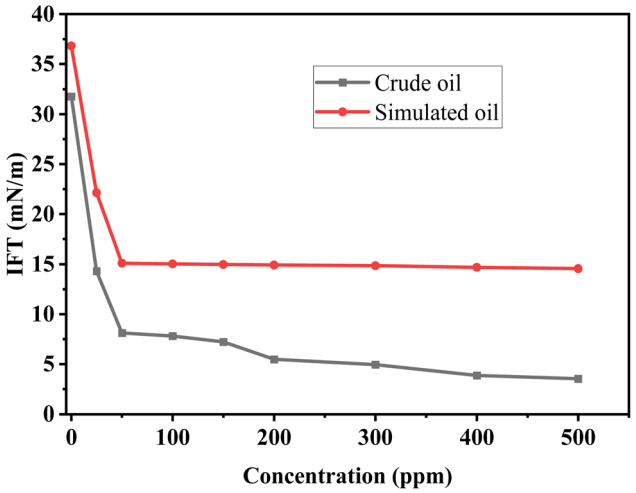

Fig. 5 Equilibrium interfacial tension as a functional of GOPH concentrations between GOPH nanofluids and crude oil/simulated oil.

asphaltenes. These components could cooperate with GOPH at the interface, further enhancing its ability to reduce the oil–water interfacial tension.

Fig. 6 presents comprehensive physical illustrations and data from the hydrophilic rock surface tests. Notably, the

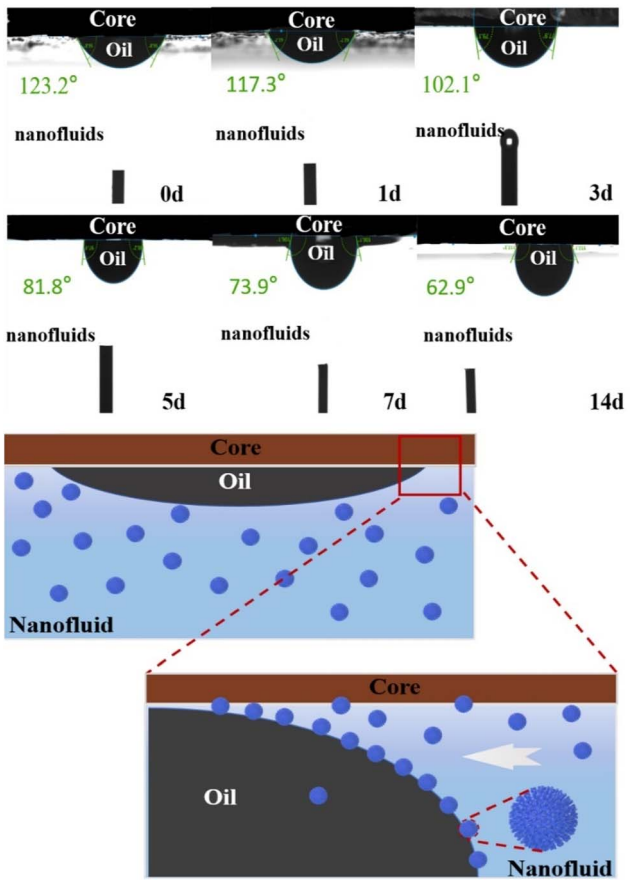

Fig. 6 Three-phase contact angles of rock surface treated by 300 ppm of GOPH nanofluids.

wettability of the oil-wet core surface underwent significant changes as the immersion time increases, a phenomenon attributed to the complex interaction between GOPH nanoparticles and the rock surface. Initially, the contact angle of 123.2° indicates the oil-wet nature of the rock core samples. However, after immersion in GOPH nanofluids (300 ppm), the contact angle gradually decreased, indicating a change in rock surface wettability. After 14 days of immersion, the contact angle of the oil-wet rock core surface reached a minimum of 62.9°, indicating the wettability of the rock surface is changing from the oil-wet state to a water-wet state. The capacity of GOPH nanoparticles to regulate rock surface wettability is closely related to their adsorption to the rock surface. Specifically, the hydrophilic groups within GOPH nanoparticles interact with the polar groups on the rock surface, resulting in adsorption and subsequent changes in the chemistry properties of the rock surface, transforming it from an oil-wet state to a water-wet state.

To investigate the behavior of GOPH nanoparticles at the oil–water interface, we adopted an intuitive experimental approach to verify the self-assembly process of GOPH nanoparticles at the interfacial oil–water film. As shown in Fig. 7, our findings show that when droplets are not allowed to remain in the oil phase for long periods of time, droplets maintain a smooth surface as the droplet is deflated or aspirated (Fig. 7a and b). This phenomenon suggests that in such instances, GOPH nanoparticles takes time to migrate to the oil–water interface and thereby cannot coalesce into a robust interfacial film. A marked transformation occurs when the droplets are immersed in the oil phase for 30 minutes. During deflation and aspiration, the oil–water interface exhibits somehow wrinkled film as the droplet size fluctuates, indicating the formation of GOPH film (Fig. 7c and d). It is worth noting that this wrinkling behavior is not very noticeable, as the size of the droplet in the experiment is much larger compared to the previous study.[12] However, this GOPH film is rigid and viscoelasticity to support the elongated droplets. Meanwhile, this rigid GOPH hinders the coalescence of the droplet, thereby effectively stabilizing the oil–water system.

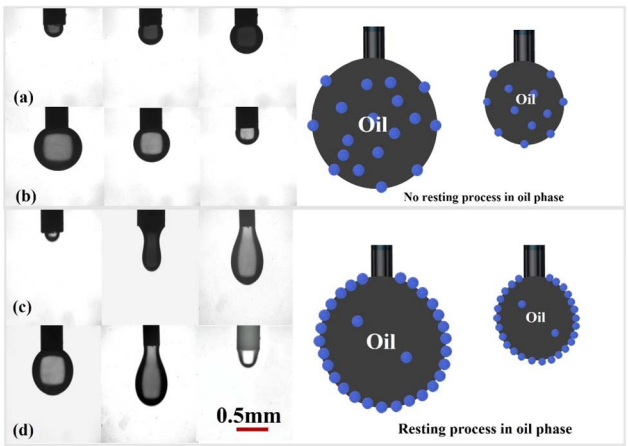

Fig. 7 Folding of interfacial membranes: (a and b) squeezing and sucking (no resting process), (c) sucking after resting and (d) squeezing after resting, GOPH nanofluids concentration of 300 ppm.

3.3 Properties of viscosity-reducing emulsions induced by GOPH

Micrographs of three fresh emulsions were prepared by stirring and mixing. A is a self-emulsion prepared by formation water and crude oil at WOR = 5/5 (water to crude oil ratio). B is an emulsion prepared by GOPH nanofluids (300 ppm) and crude oil at WOR = 5/5. B is an emulsion prepared by GOPH nanofluids (300 ppm) and crude oil at WOR = 8/2.

The experimental observations, captured under a microscope and presented in Fig. 8, reveal a distinctive W/O emulsion (emulsion A), where oil is the continuous phase and water is the dispersed phase. This emulsion exhibits a high density of droplets, arranged tightly and compactly, with an average particle size of 2.94 μm. This phenomenon is attributed to natural surfactants, such as asphaltene molecules, which facilitate the formation of W/O emulsions when mixed with formation water. Upon introducing GOPH nanoparticles, its pronounced surface activity prompts its adsorption to the oil–water interface, effectively displacing some of the asphaltenes present in the oil–water interface. This forms a complex interfacial film composed of GOPH nanoparticles and natural surfactants. This transformation converts the oil emulsion from a water-in-oil (W/O) configuration to an oil-in-water (O/W) structure. Notably, when the WOR is 5/5, the emulsion exhibits a low density of droplets with a significantly larger average particle size of 21.32 μm. However, with an increased

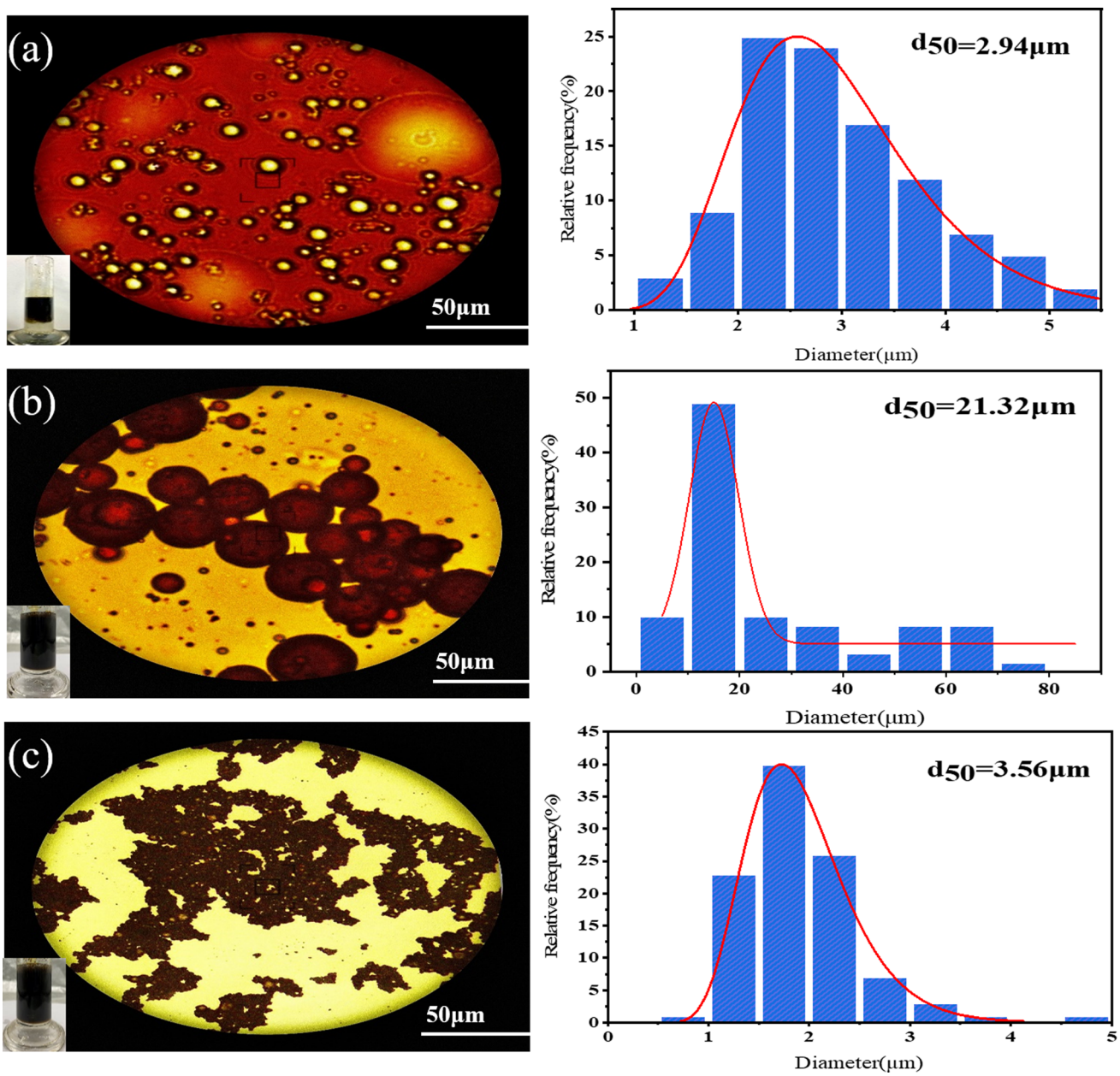

Fig. 8 Micrographs and particle size distribution of emulsions containing different chemicals: (a) brine (WOR = 5/5); (b) 300 ppm GOPH nanofluids (WOR = 5/5); (c) 300 ppm GOPH nanofluids (WOR = 8/2).

water content (WOR = 8/2), the emulsion density increases, and the particle size decreases to an average of 3.56 μm. This shift towards a smaller particle size and more homogeneous distribution of oil droplets suggests that the emulsions formed after the addition of GOPH nanoparticles are more stable and exhibit a superior emulsification effect. These findings indicate that GOPH has a synergistic effect with active components such as asphaltenes in crude oil to better promote the oil–water phase transition and improve the emulsion stability and that GOPH induces oil–water emulsification to form a viscosity-reducing emulsion with small particle sizes at high water content (80%).

As depicted in Fig. 9a, the viscosities of the three freshly prepared emulsions are presented. Notably, the viscosity of the emulsion A prepared by formation water and crude oil exceeds the viscosity of crude oil by approximately fourfold. This significant increase is primarily attributed to the formation of a water-in-oil (W/O) emulsion. Asphaltene, rich in –OH groups as potent polar moieties with notable hydrogen bonding capabilities, plays a pivotal role in enhancing the viscosity of these emulsions. Additionally, the higher content of heteroatomic compounds in asphaltene facilitates the formation of intermolecular hydrogen and covalent bonds, constructing reticulated aggregates that further bolster the emulsion's viscosity. However, upon the addition of GOPH nanoparticles, a significant reduction in emulsion viscosity is observed. At the highest WOR of 8/2, the viscosity of the emulsion approaches that of water, reaching 1.56 mPa s. This reduction can be explained by the increasing displacement of asphaltenes and the adsorption of GOPH at the oil–water interface as the WOR increases. As more GOPH is adsorbed, the viscosity further decreases.

To assess the stability of the three emulsions, we conducted a dewatering rate test, and the outcomes are presented in Fig. 9b. At reservoir temperature of 70 °C, the dehydration rate of the crude oil–water self-emulsions exhibited a rapid increase, ultimately attaining 82% after seven days. In contrast, the dehydration rates of GOPH emulsions exhibited a slower increase. Specifically, the emulsion with a WOR of 5/5 reached a dehydration rate of 22% after seven days, suggesting the poor stability of this oil-in-water (O/W) emulsion. Interestingly, the emulsion with a WOR of 8/2 began to dehydrate on the second day but exhibited a dehydration rate of only 11% after seven days, indicating good stability in high water content. These results indicate that, as the WOR increases, the emulsion becomes more stable. This phenomenon is mainly attributed to the increased adsorption of GOPH nanoparticles onto the interfacial film, which forms a composite unit with asphaltene, thereby constructing a flexible interfacial film that stabilizes the O/W emulsion.

3.4 Viscoelasticity of emulsions

The expansion complex (E) reveals the interfacial resistance to changes in the interface area, which includes a real and an imaginary component and is defined as:

$$E = E' + iE'' \quad (1)$$

where the elastic modulus E' is the real component and the viscous modulus E'' is the imaginary component. The E' is regarded as the elastic energy stored in the interface, and E'' is regarded as the loss energy.[25] Fig. 10 illustrates the frequency-dependent evolution of the viscous modulus, elastic modulus (Fig. 10a), and phase angle (Fig. 10b) for crude oil self-emulsified emulsions and emulsions induced by GOPH nanofluids over the entire frequency spectrum from 0.1 to 100 Hz. The viscoelastic properties of the oil–water self-emulsified emulsions reveals that both viscous and elastic modulus exhibit an increasing trend with frequency, with a more pronounced rise in the elastic modulus. This behavior is attributed to the interplay between droplet flow and liquid film deformation in the emulsion system, where the joint action of

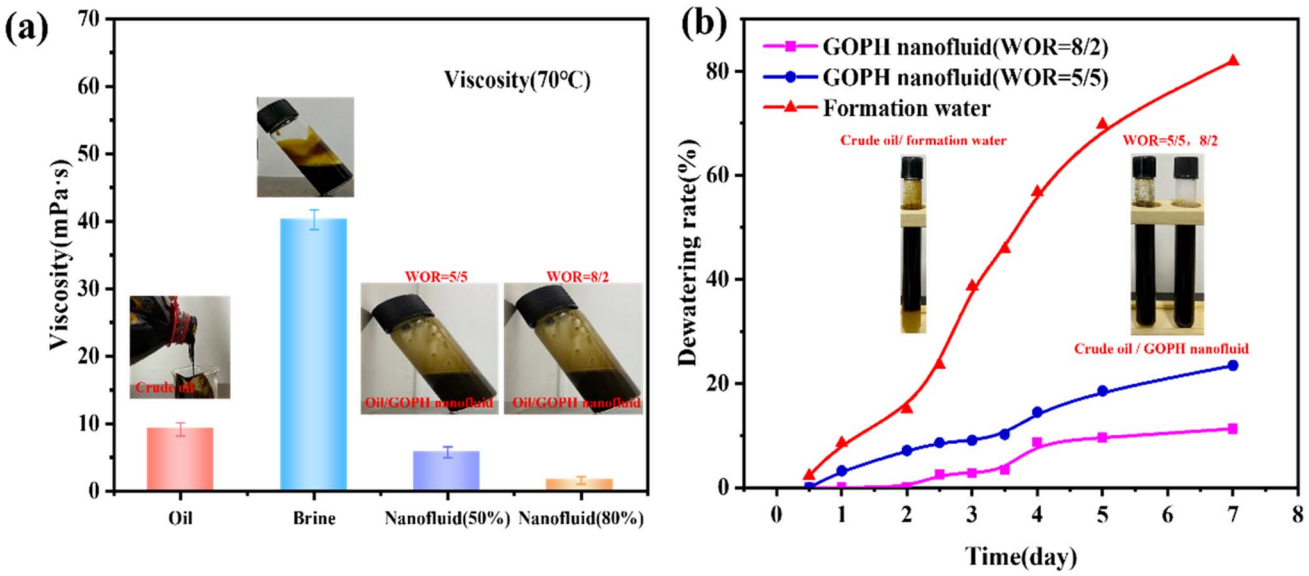

Fig. 9 (a) Crude oil and various types of emulsion viscosity testing and (b) stability evaluation.

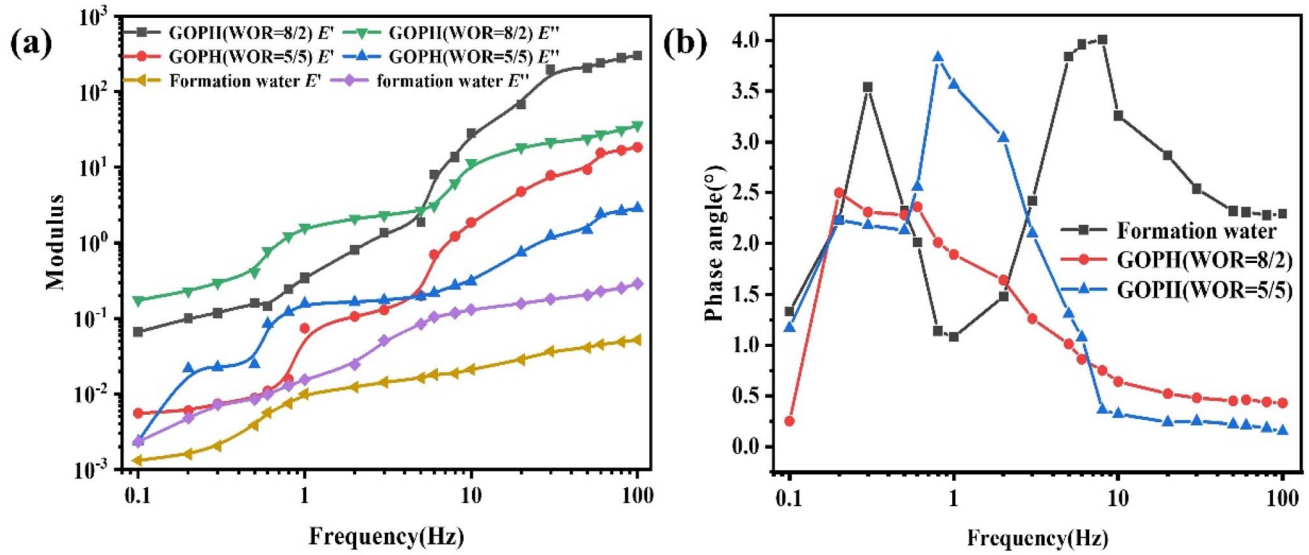

Fig. 10 Interfacial expansion modulus (a) and phase angle of various types of emulsions (b).

these processes at varying frequencies leads to distinct energy dissipation patterns, ultimately affecting the modulus values.

Additionally, the relationship between the phase angle and viscoelasticity of emulsions was illustrated to explain the viscoelasticity of emulsions.

$$E' = E\cos\theta \quad (2)$$

$$E'' = E\sin\theta \quad (3)$$

where θ is the phase angle. As frequency increases, the phase angle values for all emulsion systems exhibit a downward trend (Fig. 10b), indicating an enhancement in the elastic behavior of the emulsions. This is attributed to the deformations and orientation changes of the emulsions under external shear forces at high-frequency oscillations, resulting in a more elastic behavior. As for the crude oil self-emulsified emulsions, the viscous modulus remains consistently higher than the elastic modulus by 1 to 2 orders of magnitude in the entire frequency range, indicating that these crude oil self-emulsified emulsions primarily exhibit viscous characteristics.

However, the viscoelasticity tests of emulsions intervened with GOPH indicate that viscous and elastic modulus increase with frequency, with a more significant increase in the elastic modulus. Notably, within a specific low-frequency range, the viscous modulus exceeds the elastic modulus by an order of magnitude, reflecting the viscous nature of the emulsions. However, above this frequency threshold, the elastic modulus surpasses the viscous modulus, indicating that these emulsions induced by GOPH nanoparticles exhibit elastic properties.

3.5 Mechanism of GOPH-induced formation of viscosity-reducing emulsions in crude oil

Fig. 11 delineates the underlying mechanisms behind the GOPH-mediated formation of viscosity-reducing emulsions in crude oil. Asphaltene intermolecular interactions, primarily comprising dispersive, electrostatic, and hydrogen bonding

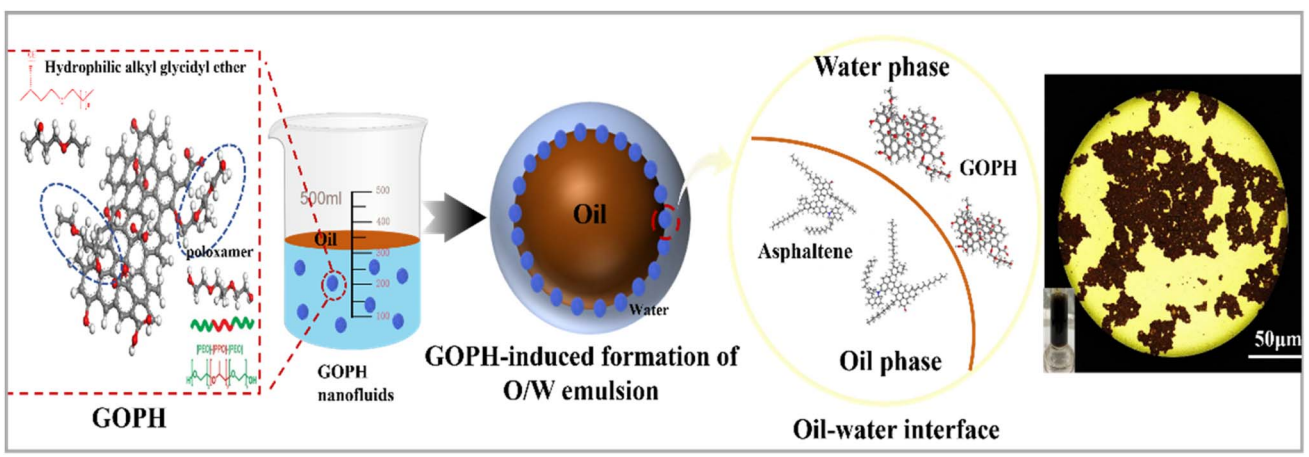

Fig. 11 Mechanism of GOPH-induced formation of viscosity-reducing emulsions in crude oil.

forces, are pivotal in augmenting crude oil viscosity by promoting nano-aggregate formation through π–π aromatic ring stacking. Notably, oil–water self-emulsification leads to the formation of W/O emulsions, where asphaltene monolayers predominantly occupy interfacial adsorption sites. Asphaltene's abundance in –OH groups, possessing robust hydrogen bonding capabilities, significantly elevates emulsion viscosity. The introduction of GOPH nanoparticles disrupt this viscosity-inducing mechanism. Specifically, GOPH synergizes with asphaltenes to produce stable O/W emulsions, ultimately reducing crude oil viscosity. This emulsification process is driven by interactions between carboxyl and amide groups of asphaltene and hydrophilic moieties of GOPH, forming an amide-GOPH-carboxylate complex unit at the oil–water interface. This complex unit replaces individual asphaltene molecules at interfacial adsorption sites, resulting in a more flexible interfacial film. Furthermore, the interfacial activity of asphaltene in the aqueous phase enables it to adsorb at the oil–water interface. GOPH nanoparticles, in turn, adsorb onto these asphaltene molecular spacers, effectively "locking" and "anchoring" the asphaltene molecules, enhancing their stability at the interface. This interaction between GOPH and asphaltene, constructs an amide-GOPH-carboxylate composite unit, which not only significantly reduces the crude oil–water interfacial tension, but also facilitates the synergistic construction of a more elastic and stable interfacial film.

4. Conclusion

A groundbreaking carbon-based nano-emulsifying agent, GOPH, synthesized using hydrophilic alkyl glycidyl ether and poloxamer modifiers, exhibits exceptional emulsification and viscosity-reducing capabilities for crude oil. GOPH significantly reduces the oil–water interfacial tension to 9.76 mN m^{-1} at a critical concentration of around 45 ppm. Interfacial film folding experiments reveal that GOPH adsorbs at the oil–water interface, forming a rigid film. A viscosity-reducing oil-in-water emulsion is induced by incorporating a small amount (300 ppm) of GOPH into the aqueous phase of ordinary thick oil. Leica microscopy and particle size analysis demonstrate a substantially reduced emulsion particle size with increasing water content. Specifically, at 80% water content, particle size reaches 1.56 μm, accompanied by a tenfold viscosity reduction and a viscosity reduction rate of 91.6%. Notably, emulsions exhibit superior stability with increasing water content, with the 80% water content emulsion maintaining a dehydration rate of only 11% after seven days of ageing. Dilatational rheology experiments confirm the viscoelastic fluid nature of the emulsion. The formation of this interfacial film is attributed to the construction of amide-GOPH-carboxylate complexes through GOPH interaction with asphaltene, which stabilizes the oil-in-water emulsion.

Data availability

All data that support the findings of this study are included within the article.

Author contributions

Writing—original draft, writing—review and editing, and FTIR analysis: W. C. and R. H.; methodology, conceptualization, and funding acquisition: R. L., J. Z. and R. L.; data curation and validation: H. W., W. G., Z. L. and B. F.; methodology and visualization: W. P. All authors have read and agreed to the published version of the manuscript.

Conflicts of interest

The authors declare that they have no competing financial interests or personal relationships that could have appeared to influence the work reported in this paper.

Acknowledgements

We acknowledge National Natural Science Foundation of China (Grant No. 42172347), Distinguished Youth Foundation of Sichuan Scientific Committee (Grant No. 2024NSFJQ0028) and for providing financial supports of this study.

References

1 Y. Xuan, Z. Zhao, D. Li, *et al.*, Recent advances in the applications of graphene materials for the oil and gas industry, *RSC Adv.*, 2023, **13**(33), 23169–23180.
2 S. Yuan and Q. Wang, New progress and prospect of oilfields development technologies in China, *Petrol. Explor. Dev.*, 2018, **45**(4), 698–711.
3 R. Liu, Y. Lu, W. Pu, *et al.*, Low-energy emulsification of oil-in-water emulsions with self-regulating mobility *via* a nanoparticle surfactant, *Ind. Eng. Chem. Res.*, 2020, **59**(41), 18396–18411.
4 S. Pang, W. Pu, J. Xie, *et al.*, Investigation into the properties of water-in-heavy oil emulsion and its role in enhanced oil recovery during water flooding, *J. Petrol. Sci. Eng.*, 2019, **177**, 798–807.
5 F. Jiao, C. Zou, Z. Yang, *et al.*, Geological theory and exploration development practice of hydrocarbon accumulation inside continental source kitchens, *Petrol. Explor. Dev.*, 2020, **47**(6), 1147–1159.
6 S. H. Habib, R. Yunus, R. Zakaria, *et al.*, Chemical enhanced oil recovery: synergetic mechanism of alkali, surfactant and polymer with overview of methyl ester sulfonate as a green alternative for EOR surfactant, *Fuel*, 2024, **363**, 130957.
7 S. Prakash, D. Joshi, K. Ojha, *et al.*, Enhanced oil recovery using polymer alternating CO_2 gas injection: mechanisms, efficiency, and environmental benefits, *Energy Fuels*, 2024, **38**(7), 5676–5689.
8 A. Kovscek, Emerging challenges and potential futures for thermally enhanced oil recovery, *J. Petrol. Sci. Eng.*, 2012, **98**, 130–143.
9 T. Telmadarreie, P. Berton, S. L. Bryant, *et al.*, Treatment of water-in-oil emulsions produced by thermal oil recovery techniques: review of methods and challenges, *Fuel*, 2022, **330**, 125551.

10 I. Kurnia, M. Fatchurrozi, R. Anwary, *et al.*, Lessons learned from coreflood experiments with surfactant-polymer and alkali-surfactant-polymer for enhanced oil recovery, *Petroleum*, 2022, **9**, 487–498.

11 J. Sun, Z. Xiu, L. Li, *et al.*, Application status and prospect of ionic liquids in oilfield chemistry, *Petroleum*, 2024, **10**, 11–18.

12 L. He, F. Lin, X. Li, *et al.*, Interfacial sciences in unconventional petroleum production: from fundamentals to applications, *Chem. Soc. Rev.*, 2015, **44**, 5446–5494.

13 X. Sun, H. Ning, G. Chen, *et al.*, Experimental study of hybrid nanofluid-alternating-CO_2 microbubble injection as a novel method for enhancing heavy oil recovery, *J. Mol. Liq.*, 2024, **395**, 123835.

14 J. J. Sheng, Status of surfactant EOR technology, *Petroleum*, 2015, **1**(2), 97–105.

15 X. Chen, Y. Li, Z. Liu, *et al.*, Visualized investigation of the immiscible displacement: influencing factors, improved method, and EOR effect, *Fuel*, 2023, **331**, 125841.

16 S. Asadabadi, J. Saien and M. Kharazi, Enhanced interfacial activity by maximizing synergy between long-chain ionic liquid and conventional surfactant for enhanced oil recovery, *RSC Adv.*, 2022, **14**(27), 18942–18949.

17 S. Chowdhury, S. Shrivastava, A. Kakati, *et al.*, Comprehensive review on the role of surfactants in the chemical enhanced oil recovery process, *Ind. Eng. Chem. Res.*, 2022, **61**(1), 21–64.

18 K. Al-Azani, S. Abu-Khamsin, R. Al-Abdrabalnabi, *et al.*, Oil recovery performance by surfactant flooding: a perspective on multiscale evaluation methods, *Energy Fuels*, 2022, **36**(22), 13451–13478.

19 S. Kalam, S. A. Abu-Khamsin, S. Patil, *et al.*, Adsorption reduction of a gemini surfactant on carbonate rocks using formic acid: static and dynamic conditions, *Fuel*, 2023, **345**, 128166.

20 S. Kalam, S. A. Abu-Khamsin, M. S. Kamal, *et al.*, Review on surfactant retention on rocks: mechanisms, measurements, and influencing factors, *Fuel*, 2021, **293**, 120459.

21 T. Amirianshoja, R. Junin, A. K. Idris, *et al.*, A comparative study of surfactant adsorption by clay minerals, *J. Petrol. Sci. Eng.*, 2013, **101**, 21–27.

22 R. Liu, J. Lu, W. Pu, *et al.*, Synergetic effect between insitu mobility control and micro-displacement for chemical enhanced oil recovery (CEOR) of a surface-active nanofluid, *J. Pet. Sci. Eng.*, 2021, **205**, 108983.

23 Y. Yang, J. Guo, Z. Cheng, *et al.*, New composite viscosity reducer with both asphaltene dispersion and emulsifying capability for heavy and ultraheavy crude oils, *Energy Fuels*, 2017, **31**(2), 1159–1173.

24 J. Zhang, H. Huang, M. Zhang, *et al.*, Experimental investigation of nanofluid enhanced oil recovery by spontaneous, *RCS Adv*, 2023, **13**(24), 16165–16174.

25 Y. Liu, C. Liu, Y. Li, *et al.*, Experimental study of an amphiphilic graphene oxide based nanofluid for chemical enhanced oil recovery of heavy oil, *New J. Chem.*, 2023, **47**(4), 1945–1953.

26 J. Sarkar, P. Ghosh and A. Adil, A review on hybrid nanofluids: recent research, development and applications, *Renewable Sustainable Energy Rev.*, 2015, **43**, 164–177.

27 B. Peng, L. Zhang, J. Luo, *et al.*, A review of nanomaterials for nanofluid enhanced oil recovery, *RCS Adv*, 2017, **7**(51), 32246–32254.

28 M. Yusuf, S. Ridha and H. Kamyab, Recent progress in NP-based enhanced oil recovery: insights from molecular studies, *J. Mol. Liq.*, 2024, **124**, 104.

29 R. Hosny, A. Zahran, A. Abotaleb, *et al.*, Nanotechnology impact on chemical-enhanced oil recovery: a review and bibliometric analysis of recent developments, *ACS Omega*, 2023, **8**(49), 46325–46345.

30 A. Amraeiniya, S. Shojaei, A. Mohseni, *et al.*, Experimental study on nanoparticles-assisted low-salinity water for enhanced oil recovery in asphaltenic oil reservoirs, *Petroleum*, 2023, **9**, 395–402.

31 R. Godiwal and M. M. Mandal, Modeling of enhanced oil recovery using nanofluid, *Chem. Eng. Technol.*, 2024, **47**(3), 568–577.

32 A. Pandey, S. F. Qamar, S. Das, *et al.*, Advanced multi-wall carbon nanotube-optimized surfactant-polymer flooding for enhanced oil recovery, *Fuel*, 2024, **355**, 129463.

33 T. Saigal, H. Dong, K. Matyjaszewski, *et al.*, Pickering emulsions stabilized by nanoparticles with thermally responsive grafted polymer brushes, *Langmuir*, 2010, **26**(19), 15200–15209.

34 R. Khoramian, S. A. A. Ramazani, M. Hekmatzadeh, *et al.*, Graphene oxide nanosheets for oil recovery, *ACS Appl. Nano Mater.*, 2019, **2**(9), 5730–5742.

35 L. Chen, X. Zhu, L. Wang, *et al.*, Experimental study of effective amphiphilic graphene oxide flooding for an ultralow-permeability reservoir, *Energy Fuels*, 2018, **32**(11), 11269–11278.

36 R. Liu, Y. Xu, W. Pu, *et al.*, Oligomeric ethylene-glycol brush functionalized graphene oxide with exceptional interfacial properties for versatile applications, *Appl. Surf. Sci.*, 2022, **606**, 154856.

37 X. Luo, P. Zheng and K. Gao, Thermo- and CO_2-triggered viscosifying of aqueous copolymer solutions for gas channeling control during water-alternating-CO_2 flooding, *Fuel*, 2021, **291**, 120171.